0022-1554/90/$3.30
The Journal of Histochemistry and Cytochemistry

Vol. 38, No. 11, pp. 1549–1563, 1990
Printed in U.S.A.

Original Article

Expression and Localization of the Two Small Proteoglycans Biglycan and Decorin in Developing Human Skeletal and Non-skeletal Tissues

PAOLO BIANCO,[1,2] LARRY W. FISHER, MARIAN F. YOUNG, JOHN D. TERMINE, and PAMELA GEHRON ROBEY

Bone Research Branch, National Institute of Dental Research, National Institutes of Health, Bethesda, Maryland 20892.

Received for publication January 13, 1990 and in revised form May 31, 1990; accepted June 14, 1990 (0A1883).

The messenger RNAs and core proteins of the two small chondroitin/dermatan sulfate proteoglycans, biglycan and decorin, were localized in developing human bone and other tissues by both ^{35}S-labeled RNA probes and antibodies directed against synthetic peptides corresponding to non-homologous regions of the two core proteins. Biglycan and decorin expression and localization were substantially divergent and sometimes mutually exclusive. In developing bones, spatially restricted patterns of gene expression and/or matrix localization of the two proteoglycans were identified in articular regions, epiphyseal cartilage, vascular canals, subperichondral regions, and periosteum, and indicated the association of each molecule with specific developmental events at specific sites. Study of non-skeletal tissues revealed that decorin was associated with all major type I (and type II) collagen-rich connective tissues. Conversely, biglycan was expressed and localized in a range of specialized cell types, including connective tissue (skeletal myofibers, endothelial cells) and epithelial cells (differentiating keratinocytes, renal tubular epithelia). Biglycan core protein was localized at the cell surface of certain cell types (e.g., keratinocytes). Whereas the distribution of decorin was consistent with matrix-centered functions, possibly related to regulation of growth of collagen fibers, the distribution of biglycan pointed to other function(s), perhaps related to cell regulation. (*J Histochem Cytochem 38:1549–1563, 1990*)

KEY WORDS: Proteoglycans; Biglycan; Decorin; In situ hybridization; Bone development; Tissue localization.

Introduction

Developing human bone contains two small chondroitin sulfate (CS) proteoglycans, biglycan (PG I) and decorin (PG II), which are the products of different genes (5). Biglycan consists of a core protein of M_r 42,510 and two CS chains; decorin has a core protein of similar size and one CS chain. The core protein sequence of cultured human bone cell decorin is identical to that of the human fibroblast protein (5,11). Biglycan core protein sequence is quite the same as that of bovine cartilage PG I (15) (with minor interspecies variations) and is distinct from, although significantly homologous with, decorin core protein sequence (5). Both PG I/biglycan and PG II/decorin are presently viewed as comprising a subset of virtually ubiquitous extracellular proteoglycans in most connective tissue matrices (7–9,15,20,21). The tissue localization of decorin (3,17,22,25,27), and its proven ability to inhibit collagen fiber growth in vitro (26) led to the postulate that it may correspond to the PG localized cytochemically to defined regions of the collagen period in intact tissues (20,23,24). Therefore, its biological functions might well be related to the regulation of assembly and growth of collagen fibers. However, the distribution and functions of biglycan are still unknown.

The objective of the present study was to define and compare the patterns of localization and gene expression of biglycan and decorin in developing human skeletal and non-skeletal tissues. The temporal and spatial patterns of expression of the two proteoglycans should provide valuable insights into molecular aspects of bone development, and a necessary frame of reference for understanding their biological functions. For this purpose, we used (a) antibodies directed against synthetic peptides corresponding to non-homologous amino acid sequences in the N-terminal regions of the two core proteins, and (b) in situ hybridization using ^{35}S-labeled RNA probes. This approach provided two independent ways of identifying the two proteoglycans in tissues and allowed for a correlation between gene expression and matrix deposition.

Materials and Methods

Tissues. Human tissues of gestational age 14–17 weeks obtained from therapeutic procedures were used for this study. The material was immediately placed in Dulbecco's minimal essential medium and dissected within 2 hr. Tissues sampled included long bones of the limbs (femur, tibia, hu-

[1] Correspondence to: Paolo Bianco, Bone Research Branch, National Institute of Dental Research, NIH, Bldg. 30, Rm. 106, Bethesda, MD 20892.
[2] Present address: Dip Biopatologia Umana, Sez Anatomia Patologica, Università 'La Sapienza,' Viale Regina Elena 324, I-00161 Roma, Italy.

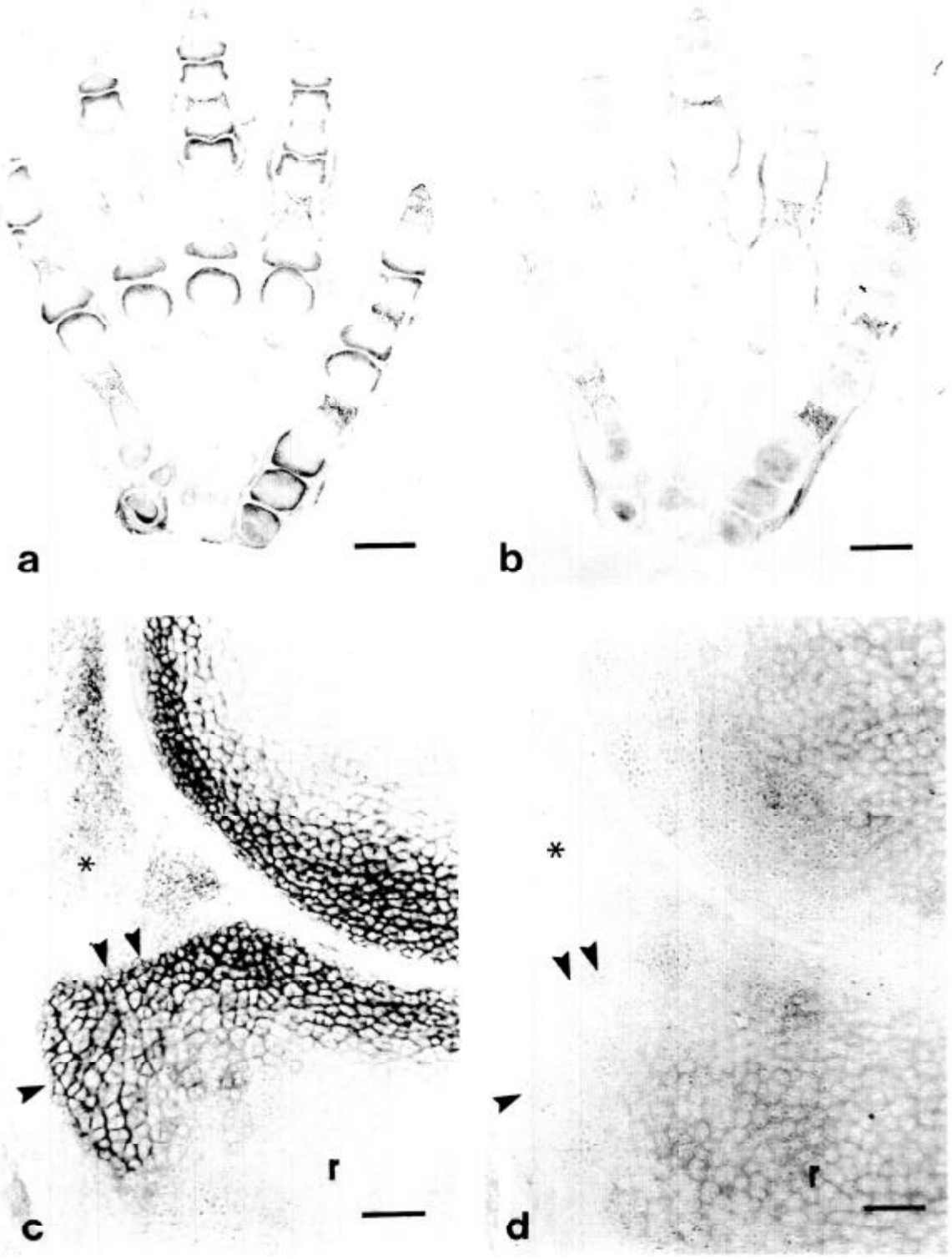
a
b
c
d
r
r

merus, and ulna), ribs, calvaria, lower jaws, viscera (kidney, adrenal, liver, lung), skin, skeletal muscle, peripheral nerves, eyes, tendons, whole hands and feet, and placenta. Tissues were fixed for 2 hr or overnight at 4°C in 4% formaldehyde (freshly made from paraformaldehyde) in 0.1 M phosphate buffer, pH 7.2. Additional samples were snap-frozen in dry ice-cooled isopentane and cryostat sectioned. Frozen sections were used for a preliminary assessment of potential loss of immunoreactivity in aldehyde-fixed, paraffin-embedded vs frozen tissues. Routine paraffin embedding of fixed material was adopted as the standard tissue preparation protocol, given the identity of immunostaining results obtained in such preliminary study and the better preservation of morphology. Bone samples were decalcified in buffered EDTA.

Antibodies. The two "peptide" rabbit antisera used in this study were described elsewhere in detail and proven to be monospecific (4,5). Briefly, antiserum LF-15 was generated against a synthetic peptide corresponding to amino acids 11–24 of the secreted form of human bone PG I/biglycan. The peptide was conjugated to BSA. Antiserum LF-30 was generated against a synthetic peptide corresponding to amino acids 5–17 of human PG II/decorin. This peptide was conjugated to keyhole limpet hemocyanin. When used in Western blot and immunoprecipitation, LF-15 recognized the core protein of PG I/biglycan, and LF-30 the core protein of PG II/decorin, with no crossreactivity (4,5).

Immunostaining. Sections mounted on poly-L-lysine-coated slides were deparaffinized, treated with chondroitin ABC lyase (see below), and exposed to 0.3% hydrogen peroxide for 30 min. After washing in PBS, the sections were exposed to a 1:5 dilution of normal goat serum for 30 min and then incubated with a 1:200 dilution of the primary antiserum in PBS, 0.1% BSA for 2 hr. The sections were then washed in PBS, 0.01% Triton X-100 (four times for 10 min), and incubated with a 1:100 dilution of an affinity-purified, peroxidase-labeled goat anti-rabbit IgG antibody (Kirkegaarde and Perry; Rockville, MD) for 30 min. After washing in PBS–Triton X-100, the sections were reacted with 3,3'-diaminobenzidine and hydrogen peroxide (6), rinsed in distilled water, dehydrated in ascending concentrations of ethanol, cleared in xylene, and mounted in Permount. Sections were counterstained with hemalum as needed. All incubations were done at room temperature except the ABCase digestion described below.

Chondroitinase Digestion. Because the peptide antibodies quantitatively recognize protein cores devoid of attached glycosaminoglycan chains, sections were treated with chondroitin ABC lyase (protease-free, from *Proteus vulgaris*; ICN Biochemicals, Covina, CA) before immunostaining. Several concentrations of ABCase, ranging from 0.01 to 2.5 U/ml in 0.1 M Tris, 0.05 M calcium acetate, 0.01% BSA, pH 7.2, for 10 min at 37°C were assayed before adopting 1.25 U/ml as the standard.

Control of Immunostaining. Control of immunostaining included substitution of normal rabbit serum (1:200) for primary antisera, and antigen absorption tests. These were done by incubating 1 nanomole of each peptide with 100 µl of the highest working dilution of the primary antibody overnight at 4°C, followed by centrifugation at 10,000 × g for 5 min, and use in immunostaining. Each antibody was also incubated with the noncorresponding peptide to check specificity of the absorption.

Preparation of RNA Probes. The templates used for transcription were (a) a pBluescriptSK plasmid (P16) containing a 1658 BP insert with the complete protein-encoding sequence of human bone biglycan, and (b) a pBluescriptSK plasmid (P2) containing a 1.6 KB insert with the protein-encoding sequence of human bone decorin (5), identical to that described for human fibroblast decorin by Krusius and Ruoslahti (11). ^{35}S-Labeled single-stranded RNA probes (specific activity 2 × 10^8 cpm/µg) were synthesized using [^{35}S]-UTP (New England Nuclear, Boston, MA) in T3- or T7-primed reactions. Transcription conditions were as indicated by the manufacturer (Riboprobe Gemini System; Promega, Madison, WI) Both anti-sense and sense (control) probes were synthesized after linearization of the plasmids followed by phenol extraction and ethanol precipitation. For synthesis of biglycan anti-sense probe, the plasmid was linearized with Kpn I and T3-primed RNA polymerase reaction was used. The sense strand was synthesized using T7-primed RNA polymerase after linearization of the plasmid with Xba I. Decorin anti-sense was synthesized using T7-primed RNA polymerase after linearization with Bam HI; the sense strand was obtained using T3 polymerase after linearization with Kpn I. The template was removed with DNAse 1, and the probe was purified by centrifugation on a Sephadex G-50 "spin" column, and reduced in size by limited alkaline hydrolysis (1).

In Situ Hybridization. Deparaffinized sections were treated with 0.2 N HCl, digested with proteinase K (from *Tritirachium album*; Sigma, St Louis, MO), 1 µg/ml in 10 mM Tris, 2 mM $CaCl_2$ for 15 min at 37°C, washed in PBS, and acetylated in 0.25% acetic anhydride in 0.1 M triethanolamine, pH 8.0. The sections were then washed in PBS, then in 2 × SSC, dehydrated in ascending concentrations of ethanol, and air-dried. The hybridization mixture consisted of 50% formamide, 0.3 M NaCl, 20 mM Tris HCl, pH 8.0, 1 mM EDTA, 1 × Denhardt's solution, yeast tRNA 500 µg/ml, 10 mM DTT, and 10% dextran sulfate. Final probe concentration was 2 × 10^4 cpm/µl. Aliquots of the mixture sized on the dimensions of the sections were applied, and the sections were covered with small plastic squares cut out of heat-sealable "Seal-a-meal" pouches. The slides were hybridized overnight at 52°C in a humid atmosphere. The next day, the plastic squares were removed by immersing the slides in 50% formamide, 0.3 M NaCl, 20 mM Tris HCl, pH 8.0, 1 mM EDTA, 1 × Denhardt's, 10 mM dithiothreitol. The slides were then sequentially washed in 50% formamide, 4 × SSC, 10 mM DTT at 52°C for 30 min, 50% formamide, 2 × SSC, 10 mM DTT at 52°C for 30 min, 2 × SSC (four times for 5 min) at room temperature. Adventitiously bound probe was removed by digesting the sections with 20 µg/ml RNAse A, 1 µg/ml RNAse T1 in 0.5 M NaCl, 10 mM Tris HCl, pH 8.0, 1 mM EDTA, for 30 min at 37°C. The slides were then washed in RNAse buffer, then in 2 × SSC, 10 mM DTT for 30 min at room temperature, then in 0.1 × SSC, 10 mM DTT at 52°C for 15 min, 2 × SSC for 10 min at room temperature, dehydrated, and air-dried. For autoradiography, the slides were dipped in a 1:1 dilution of Kodak NTB-2 emulsion, allowed to rest vertically at room temperature for 5 hr, then exposed at 4°C for 3–8 days in the presence of desiccant. Exposed slides were developed in Kodak D-19 developer for 2.5 min at 15°C, stopped in 1% acetic acid, fixed in Kodak fixer, washed in running tap water, counterstained with hemalum, dehydrated in ethanol, cleared in xylene, and mounted in Permount. The slides were viewed in both brightfield and darkfield microscopy.

Figure 1. Sections of the whole hand of a 14-week-old human fetus stained for (**a**) biglycan and (**b**) decorin core proteins. The articular ends of each bone rudiment show a "cap" of articular cartilage that stains intensely for biglycan and remains unstained for decorin. Deeper to this zone, resting nonarticular cartilage of each epiphysis stains significantly for decorin and weakly for biglycan. Strong staining of unmineralized, newly deposited osteoid is seen in the midshaft of each rudiment. Details of the fifth metacarpo–phalangeal joint. Note absence of staining for decorin (**d**) in the biglycan-rich articular cartilage (arrowheads), and the waning of biglycan staining (**c**) in the deep, decorin-rich resting cartilage (r). Also note that articular soft tissues (asterisk), like articular cartilage, stain for biglycan and do not stain for decorin. Bars: **a,b** = 1 mm; **c,d** = 50 µm.

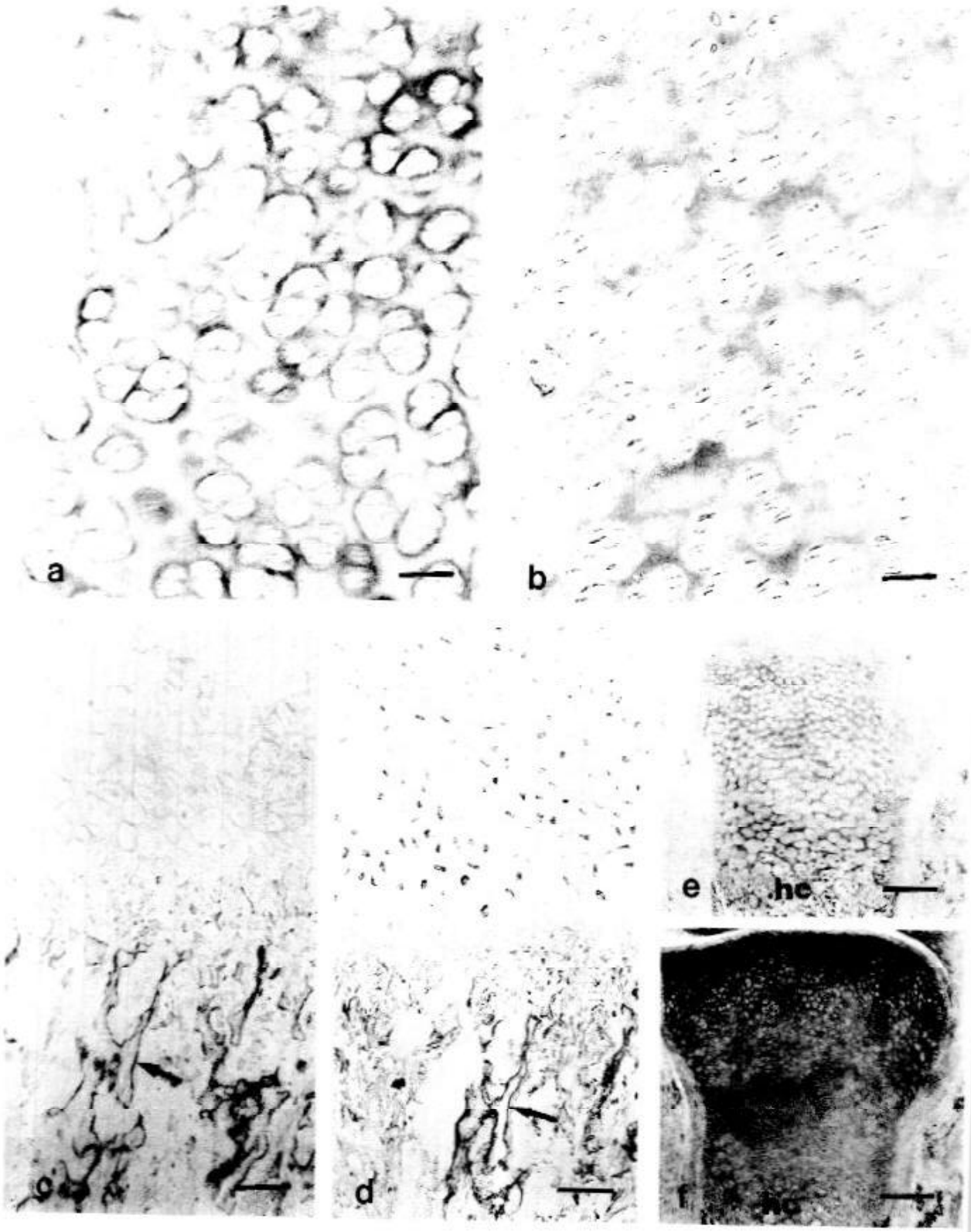
a
b
c
d
e
hc
f

Results

Immunolocalization of Biglycan and Decorin Core Proteins

Skeletal Tissues. Biglycan and decorin core proteins were specifically localized to cartilaginous and bony components of developing bones. However, important differences in the two staining patterns were noted at particular sites. Figure 1 shows the localization of biglycan and decorin core proteins in developing diarthrodial joints. Biglycan core protein was localized to an outer "cap" of prospective articular cartilage at each epiphyseal end of bone rudiments. Decorin was not detected at these sites but was found in the more deeply located nonarticular resting cartilage, in which staining for biglycan was conversely weak. Articular soft tissues (articular capsule, synovium) displayed the same staining profile as articular cartilage, i.e., they stained for biglycan but not for decorin. This mutually exclusive staining pattern in articular regions was essentially the same in all long bones studied. However, nonarticular resting cartilage stained somewhat more prominently for biglycan in limb long bones than in metacarpal and phalangeal rudiments. A halo of cartilage matrix that remained unstained for either biglycan or decorin core protein was consistently observed around vascular canals ingrowing from the perichondrium to epiphyseal cartilage of long bones.

Because endochondral ossification begins at different times and proceeds at different rates in different bone rudiments, a spectrum of developmental stages of growth plates was displayed by the different bone rudiments included in this study. At the gestational age examined, long bones of limbs were fully ossified in their diaphyseal portions, and their metaphyseal growth plates were extensively invaded by marrow vasculature and ossifying. In contrast, most developing vertebrae consisted of entirely cartilaginous rudiments, each displaying a centrally located, forming primary center of ossification. This consisted of a central area of cartilage hypertrophy surrounded by concentrically arranged proliferating chondrocytes. Metacarpal and phalangeal rudiments showed periosteal ossification in their mid-diaphysis, with variable degrees of invasion and ossification of the underlying hypertrophic cartilage. A feature common to all growth plates was a highly segregated staining pattern in the upper proliferative zone, where biglycan was restricted to territorial capsules of isogenic groups of chondrocytes (Figure 2a), and decorin to interterritorial matrix (Figure 2b). In limb long bones, matrix staining for either biglycan or decorin was virtually absent in lower proliferative, hypertrophic, and mineralizing zones of the growth plates (Figures 2c and 2d). In contrast, the corresponding zones of more immature growth plates (metacarpal, phalangeal, vertebral) showed prominent staining for decorin and less intense but distinct staining for biglycan (Figures 2e and 2f). Chondrocytes stained prominently for decorin in all growth plates, irrespective of the stainability of the matrix, whereas cellular staining for biglycan was less prominent. This was also true in other zones of cartilage, possibly indicating poorer accessibility of the intracellular biglycan core protein as opposed to the intracellular decorin core protein. Newly deposited bone matrix stained intensely for both biglycan and decorin at all sites of bone formation, of either membranous, perichondral, periosteal, or endochondral origin. Biglycan, but not decorin, was also localized to the thin layer of unmineralized matrix lining osteocytic lacunar walls and canalicular spaces.

Non-skeletal Tissues. A survey of a variety of non-skeletal tissues revealed a substantially divergent distribution of biglycan and decorin core proteins (Table 1). Whereas decorin was localized in all classical connective tissue matrices, staining for biglycan was either minor or absent in most such tissues (such as dermis, tendon, or cornea), with few exceptions (e.g., adventitia of large blood vessels, inner part of the sclera). Biglycan core protein was instead localized to a few specialized connective tissues where decorin was not detected (e.g., endocardium, articular capsules), and to a spectrum of specialized cell types of either connective tissue or epithelial nature. These included endothelial cells, skeletal myofibers, keratinocytes, and renal tubular epithelia. Developing kidney and skin provide suitable examples of the divergence of the localization patterns observed. In skin (Figure 3), decorin core protein was localized to

Table 1. *Distribution of biglycan and decorin core proteins and mRNAs in non-skeletal tissues*

Tissue	Biglycan	Decorin
Kidney	Endothelia Collecting tubules	Interstitium
Heart	Endocardium Some myocardial fibers	Subpericardium
Lung	"Small" interstitium	"Small" and "large" interstitium
Liver	–	Perisinusoidal connective tissue
Adrenal gland	Endothelia	–
Aorta	Intima Media Adventitia	Media Adventitia
Skin	Epidermis Endothelia	Dermal matrix
Tendon	–	+
Skeletal muscle	Myofibers	Connective tissue sheaths
Eye	Sclera (inner part)	Sclera Cornea
Peripheral nerve	Endothelia	Connective tissue sheaths
Placenta	Endothelia	Connective tissue core of villi

Figure 2. Epiphyseal cartilage of the humerus, upper proliferative zone. Adjacent sections stained for (**a**) biglycan and (**b**) decorin. Territorial capsules of isogenic groups of chondrocytes stain for biglycan but not for decorin. Interterritorial matrix stains for decorin but not for biglycan. (**c,d**) Same sections as in **a** and **b**, growth plates. Note that the cartilage matrix does not stain significantly for either (**c**) biglycan or (**d**) decorin. The cartilage cores of developing bone trabeculae also fail to stain, whereas newly deposited osteoid at their surfaces does stain (arrows). **e,f** show, for comparison, metacarpal rudiments, stained for (**e**) decorin and (**f**) biglycan. The hypertrophic cartilage in their growth plates (hc), at variance with that of the humeral growth plate, does stain. Note cell staining for decorin in **b** and **d**. Bars: **a,b** = 30 μm; **c,d** = 60 μm; **e,f** = 100 μm.

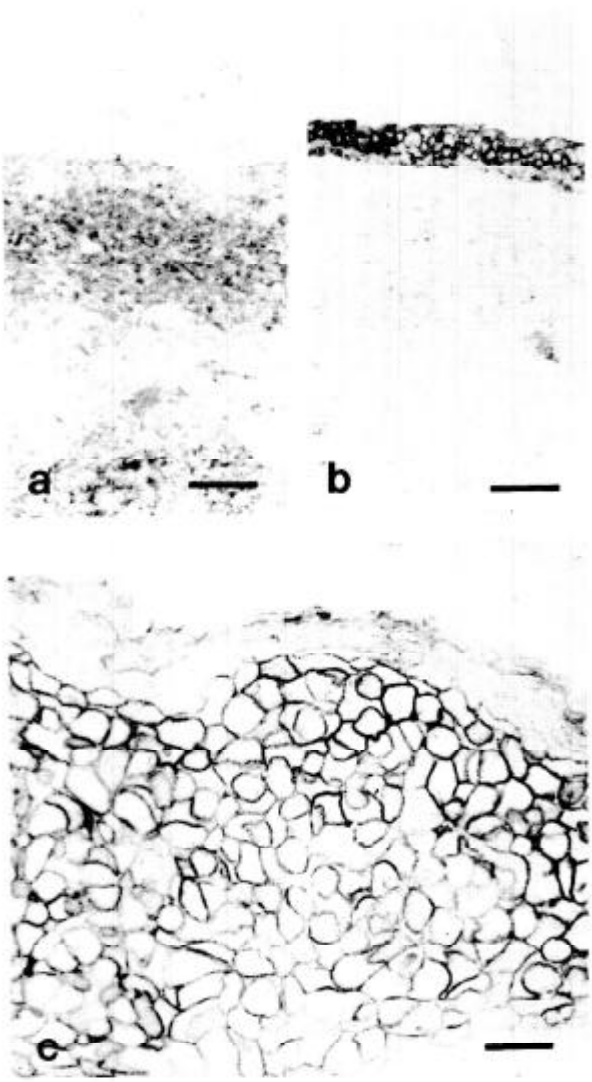

Figure 3. Immunolocalization of biglycan and decorin core proteins in fetal skin. (a) Decorin is localized to the collagenous matrix of the dermis, where staining for (b) biglycan is absent. Biglycan core protein is localized to the epidermis, where decorin is not detected. (c) Localization of biglycan core protein at the cell surface of differentiating keratinocytes. Bars: a,b = 20 μm; c = 30 μm.

the dermal collagenous matrix, whereas biglycan core protein was localized to the cell surface of differentiating keratinocytes of the prickle cell layer and, in the dermis, was restricted to the endothelial lining of capillaries. In kidney (Figure 4), decorin was localized to the interstitial connective tissue, with focal concentrations around tubular structures and at the adventitia of arteries, whereas biglycan was localized to endothelial cells and to the apical surface of epithelial cells lining collecting tubules. Occasional cells inside the glomeruli, possibly mesangial cells, also stained for decorin. Very occasionally, epithelial cells of the parietal epithelium of developing glomeruli exhibited some staining for biglycan.

Expression of Biglycan and Decorin mRNAs

Developing Bones. Although both biglycan and decorin genes were expressed in cartilage and bone cells, important differences were noted at specific regions of developing bones. High levels of biglycan mRNA were detected in articular regions (Figure 5a), in forming growth plates (such as in developing vertebrae; Figure 6a), and in perichondrium-derived mesenchymal cells inside vascular canals (Figure 7c). In contrast, low levels of decorin mRNA were found in articular cartilage (Figure 5b), whereas very high levels were detected in a narrow rim of cartilage at peripheral subperichondral locations (Figure 6b) and in chondrocytes arranged around vascular canals ingrowing from the perichondrium to epiphyseal cartilage (Figures 7a and 7b). In growth plates of limb long bones, low levels of biglycan and low or undetectable levels of decorin were observed in proliferating cartilage, and high levels of both mRNAs in hypertrophic chondrocytes (Figure 8).

In bone (Figure 9), biglycan and decorin mRNAs were co-expressed at high levels in osteoblasts on bone surfaces and in osteocytes (in the latter, biglycan was more consistently and abundantly expressed than decorin). Biglycan mRNA was not expressed significantly in fibroblasts of the outer periosteum but was abundant in pre-osteogenic cells of the inner (cambial) layer. More cell layers expressed high levels of biglycan mRNA at the metaphyseal leading edge of periosteal ossification (i.e., at the site of earliest periosteal bone formation) than at the level of the midshaft (where ossification is more advanced). Decorin mRNA, in contrast, was expressed at essentially similar levels throughout the periosteum, i.e., no difference in the levels of decorin expression could be noted between fibroblasts of the outer periosteum and pre-osteogenic cells of the cambial layer.

Non-skeletal Tissues. In non-skeletal tissues, the pattern of biglycan and decorin gene expression coincided with that of core protein localization, confirming the expression of decorin in all typical fibrous connective tissues and of biglycan in a range of specialized, epithelial, and connective tissue cell types. In skin, decorin mRNA was localized at high levels in the dermis, with substantial concentrations of grains around developing hair follicles. Biglycan mRNA, in contrast, was detected in differentiating keratinocytes (Figures 10a and 10b) and in endothelial cells of dermal capillaries (Figures 10c and 10d). In kidney (Figure 11), a strong signal for decorin was seen over the interstitium but not over tubular and

Figure 4. Localization of biglycan and decorin core proteins in developing kidney. (a,b) Low-power views of adjacent sections showing the staining of renal interstitial connective tissue for (b) decorin but not for (a) biglycan. Arrows in a and b point to the cross-sections of the same small artery. Note the staining of its endothelial lining for biglycan and of its adventitia for decorin. (c) Immunolocalization of biglycan; detail of inner cortex showing labelling of glomerular (large arrowheads) and extraglomerular (small arrowheads) capillaries, and of the luminal surface of epithelial cells lining cortical collecting tubules (arrows). (d) Immunolocalization of decorin; detail of inner cortex showing staining of interstitial connective tissue, strong staining of the adventitia of an artery (arrows), and lack of staining of glomeruli (g). Bars: a,b = 210 μm; c,d = 60 μm.

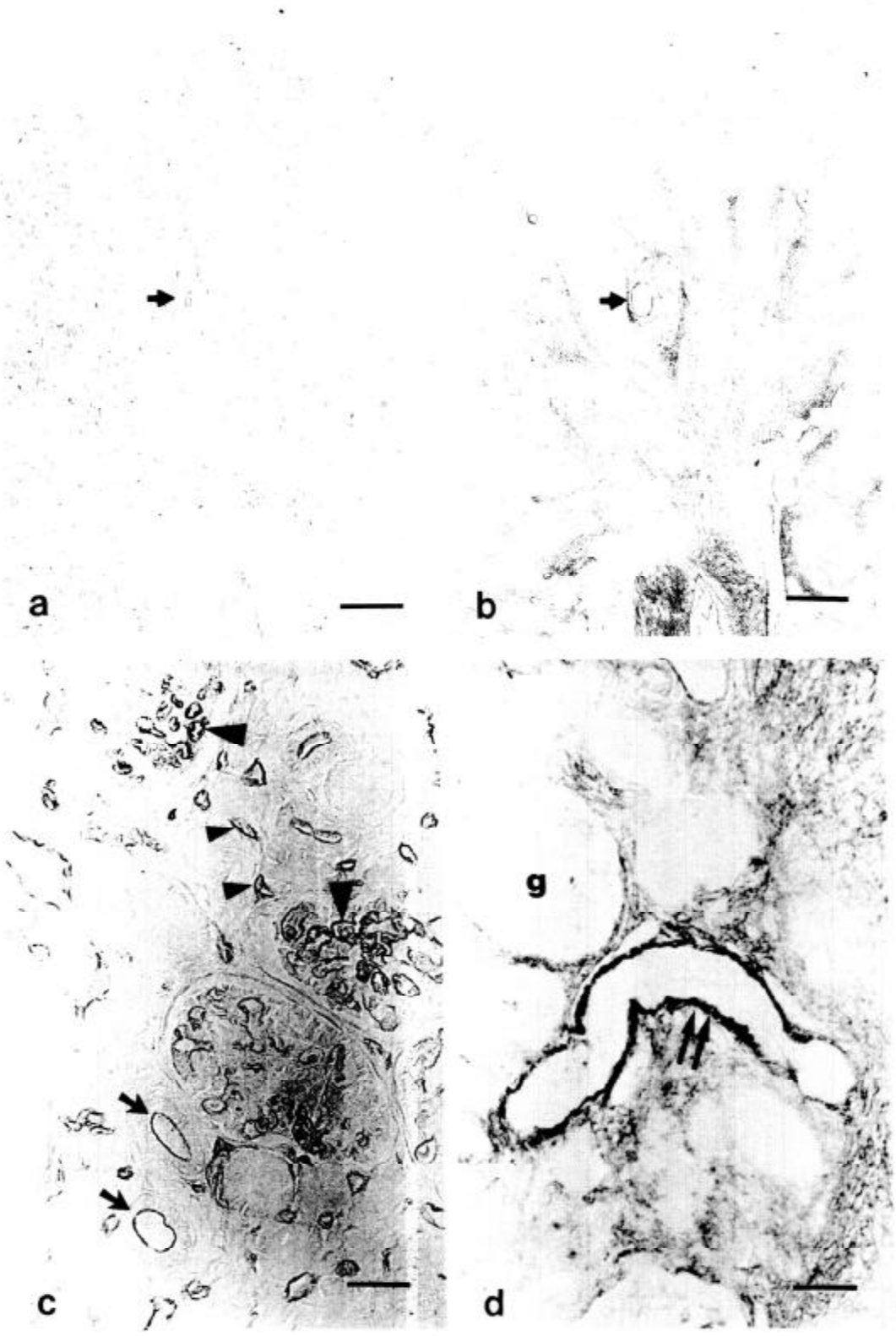
a
b
c
d
g

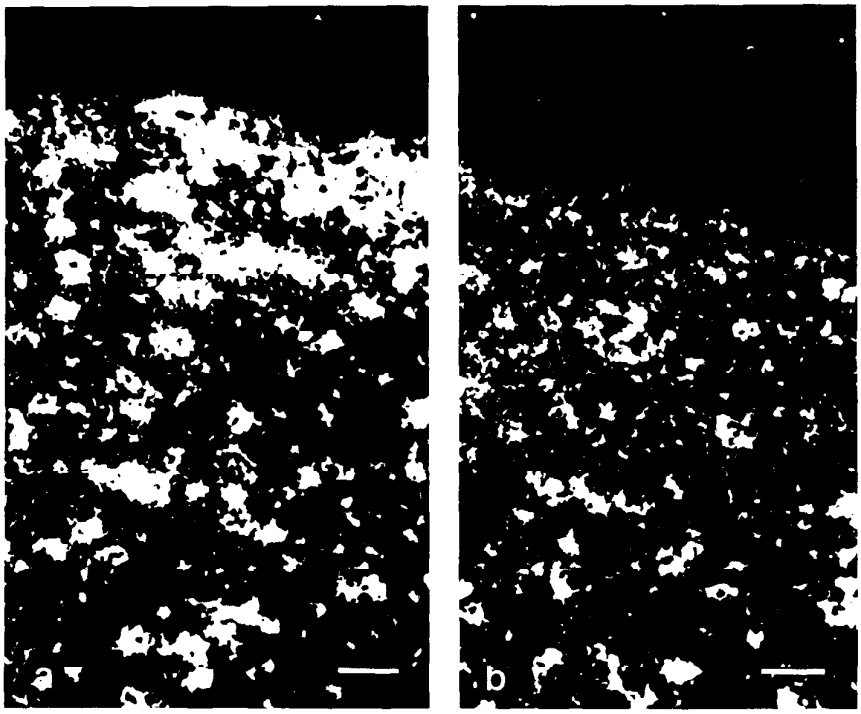

Figure 5. Localization of biglycan and decorin mRNAs in articular cartilage of the humerus. (**a**) Superficial chondrocytes show higher levels of biglycan mRNA than of (**b**) decorin mRNA. High levels of decorin mRNA are seen in deeper chondrocytes. Darkfield images. Bar = 40 μm.

glomerular structures. Biglycan mRNA was detected in glomeruli and in epithelial cells of collecting tubules. Biglycan mRNA was detected in some skeletal myofibers (Figure 12), thus confirming data from immunolocalization of the corresponding core protein.

Discussion

Using both sequence-specific "peptide" antibodies and in situ hybridization, we have presented evidence that the two small chondroitin/dermatan sulfate proteoglycans biglycan and decorin dif-

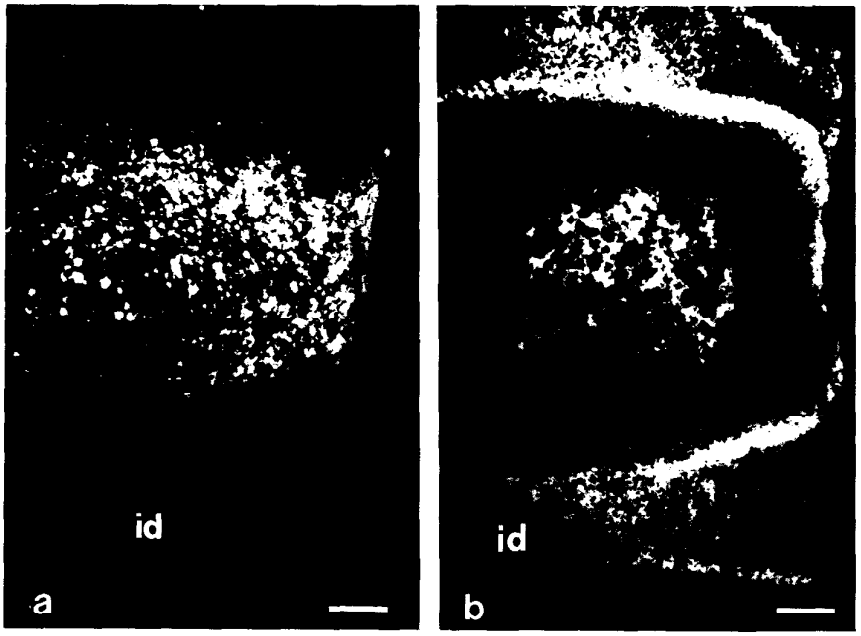

Figure 6. Developing vertebral column, darkfield images of autoradiographies of adjacent sections hybridized with (**a**) biglycan and (**b**) decorin probes. Strong hybridization signal for biglycan is detected over chondrocytes lying in an ovoid central portion of the vertebral rudiment. This "centrum" corresponds to the forming primary center of ossification, consisting of a central zone of cartilage hypertrophy surrounded by concentrically arranged layers of proliferating cells. Resting cartilage outside of this area is virtually unlabeled, as are the intervertebral discs (id). In contrast, strong hybridization signal for decorin is seen in a peripheral "shell" of resting cartilage, including forming endplates and subperichondral regions. Intervertebral discs also show hybridization signal (in both annulus and nucleus). Significant labeling is also seen in hypertrophic cartilage. Bars = 250 μm.

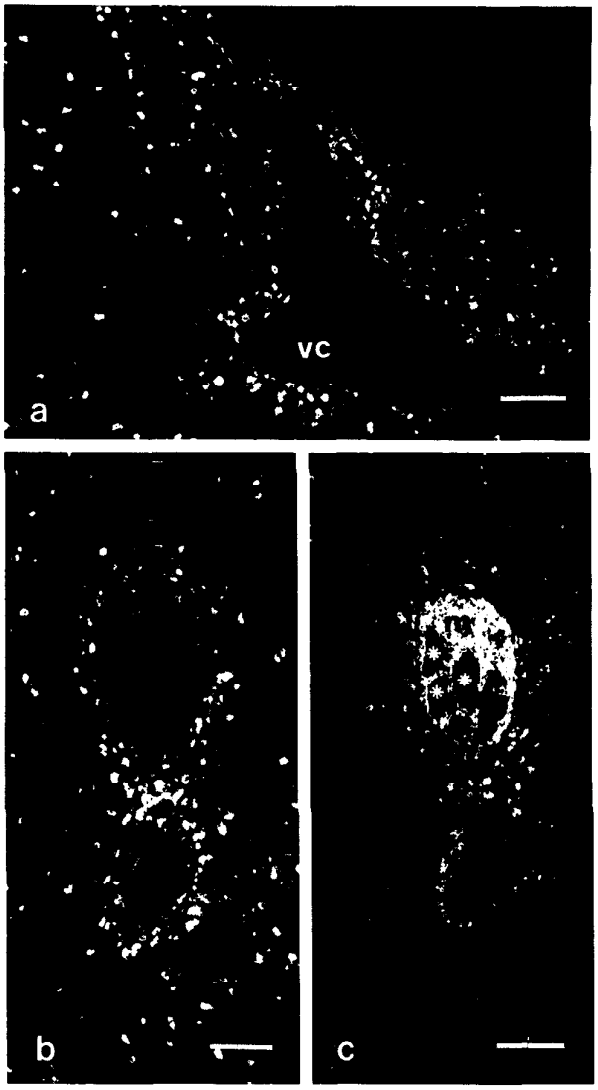

Figure 7. Expression of the biglycan and decorin genes in vascular canals of cartilage. (**a**) A vascular canal ingrowing from the perichondrium (vc) is surrounded by chondrocytes exhibiting strong hybridization signal for decorin. Chondrocytes with comparable high levels of decorin mRNA are seen scattered in the surrounding resting cartilage. (**b,c**) Adjacent sections of epiphyseal vascular canals hybridized with (**b**) decorin and (**c**) biglycan probes. Note the concentration of chondrocytes with high levels of decorin mRNA around the canal. Inside the canal, the walls of individual blood vessels (asterisks) and perichondrium-derived mesenchymal cells (m) show strong hybridization signal for biglycan but not for decorin. Bars = 80 μm.

fer significantly in distribution in developing human skeletal and non-skeletal tissues.

In developing bones, the immunolocalization of the two core proteins differed in regions of cartilage matrix known to differ significantly in morphology and overall collagen organization (e.g., articular vs non-articular regions, territorial vs interterritorial matrices). In addition, the spatial patterns of maximal expression of the two genes point to their association with specific developmental events. For example, biglycan gene was expressed at high levels in pre-osteogenic cells both in the periosteum and in morphologically undifferentiated mesenchymal cells in vascular canals, thought to be perichondrium-derived pre-osteogenic cells recruited for the formation of the secondary (epiphyseal) center of ossification (13). Decorin expression, in contrast, was not detected inside vascular canals, and was found to be uniform throughout osteogenic and non-osteogenic layers of periosteum. This suggests specific association of biglycan (but not decorin) expression with osteoblast differentiation. Furthermore, the highly segregated pattern of expression of the two genes in early bone rudiments, such as in developing vertebrae, indicates the association of the expression of the two genes with different modes of growth of individual rudiments. Decorin is maximally expressed at the sites of appositional growth (e.g., subperichondral regions), whereas biglycan expression predominates at the site of formation of growth plates. The demonstration of high levels of decorin in perivascular chondrocytes in epiphyseal cartilage may be functionally equated to the high levels of expression of decorin in subperichondral regions. In fact, the anatomical continuity of vascular canals with the perichondrium makes perivascular cartilage an internal subperichondral region in epiphyseal cartilage.

At two sites in cartilage, the combined use of in situ hybridization and immunolocalization disclosed a lack of coincidence between gene expression and matrix deposition. In a rim of cartilage matrix around vascular canals and in hypertrophic cartilage of growth plates of long bones, high levels of gene expression contrasted with the absence of stainable core proteins in the matrix. This can be explained with a negative translational control or, alternatively, with high rates of proteoglycan removal from the matrix at those particular sites. The known occurrence of degradation of cartilage matrix components both around vascular canals (12,13) and in growth plates (14) supports the second explanation. Interestingly, close contiguity with vasculature is a common feature of areas of unstainable matrix, both around vascular canals and in growth plates of long bones. In metacarpal, phalangeal, and vertebral growth plates, which were uninvaded or poorly vascularized, the matrix of growth plates did stain, at variance with growth plates of long bones, and in accordance with the high levels of biglycan and decorin transcripts in hypertrophic chondrocytes indicated by in situ data. The occurrence of different rates of PG degradation in growth plate cartilage matrix correlated with the extent of vascular invasion, appears a plausible explanation with which our in situ and immunolocalization data would be consistent.

Using a monoclonal antibody to DS/PG II, Poole et al. (17) described the presence of decorin in bovine fetal and non-fetal articular cartilage and the absence of this molecule from proliferating and hypertrophic growth plate cartilage. Our data partially match such previous findings, but reveal an outermost zone of decorin-free, biglycan-enriched cartilage matrix in human fetal prospective articular cartilage. Biochemical studies have described the presence of decorin in human articular cartilage (19,20). However, these studies focused on postnatal articular cartilage and are less directly comparable with ours, because sampling for biochemical studies and direct tissue immunolocalization obviously differ in their power of spatial resolution. Our data on the distribution of decorin out-

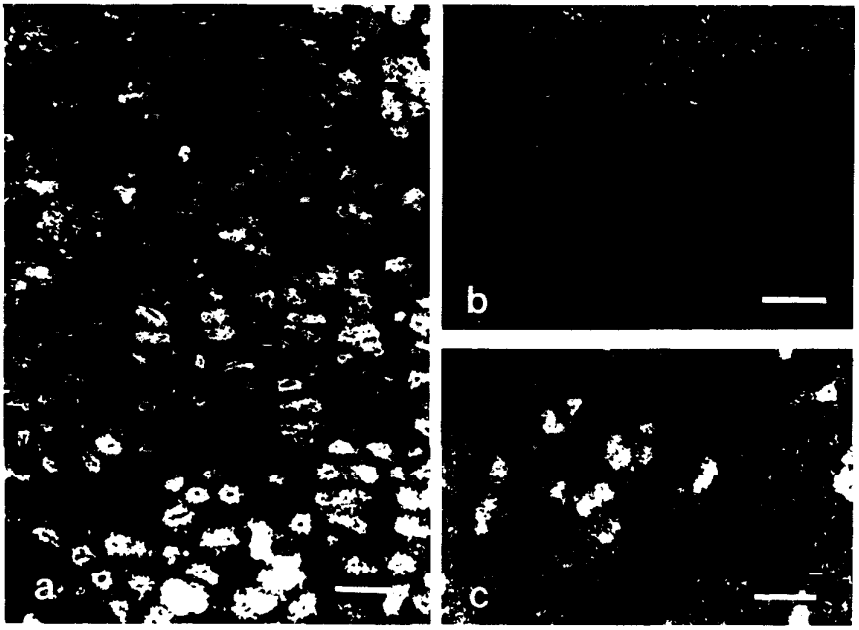

Figure 8. Detection of biglycan and decorin mRNAs in the growth plate of a long bone (femur). (**a**) Low but distinct levels of biglycan mRNA are seen in the proliferative zone (top), and strong signal is seen over hypertrophic chondrocytes (bottom). (**b**) An area of hypertrophic cartilage hybridized with a biglycan sense (control) probe. (**c**) Hypertrophic chondrocytes showing strong signal for decorin mRNA. Bars = 50 μm.

side of skeletal tissues match those previously reported by Poole et al. (17). In essence, we found decorin to be highly enriched in all collagen type I-rich connective tissues. Biglycan, in contrast, appears to be essentially absent from some typical connective tissue matrices, such as dermis, tendon, and cornea, and is expressed in a variety of unrelated cell types not involved in the production of type I collagen. In addition to some specialized connective tissue cell types, (endothelial cells, skeletal myofibers), these include epithelial cells such as keratinocytes and renal tubular epithelia, in which biglycan (or its core protein, regardless of the type, if any, of glycosaminoglycan chain) appears to be a cell surface-associated molecule. Although there is previous biochemical evidence for the production of small DS/CS proteoglycans by endothelial cells (10) and skeletal muscle (16), no precise indication existed as to their identity. Keratinocytes have been shown to produce a membrane-associated large CS proteoglycan in intact tissue (2), and also smaller proteoglycan species in culture (18). Both gene expression and localization of biglycan core protein in epidermal cells are restricted to differentiating keratinocytes (prickle cell layer) and are not detected in the proliferating cells of the basal layer. This is of interest given the change in cell/matrix interaction that represents the prerequisite for upward dislocation of epidermal cells as they shift from a proliferative to a differentiative phase of their lifespan.

Whereas the distribution of decorin lends support to its postulated function of regulation of collagen fiber assembly and growth, the distribution of the closely related biglycan strongly indicates a different biological role. The diversity of cell types expressing biglycan suggests a range of functions specific to each cell. For example, expression in skeletal myofibers would be consistent with the involvement of small PGs in the physiology of the neuromuscular junction (16). Also, given (a) the high homology of biglycan core protein with glycoprotein Ib (5), which in platelets binds von Willebrand factor, and (b) the known occurrence of synthesis and storage of von Willebrand factor in endothelial cells, the expression of biglycan by microvascular endothelia suggests potential binding of von Willebrand factor by biglycan in endothelial cells, a testable hypothesis relevant to the regulation of clot formation. However, biglycan is also homologous to gene products regulating morphogenesis in *Drosophila* (5). It is interesting, therefore, that active morphogenesis and differentiation were a common denominator of all tissues displaying biglycan expression in this study.

Whatever the ultimate function of biglycan may be, the differences in tissue distribution of biglycan and decorin are even more remarkable if matched to the similarity they share in terms of overall structure and core protein sequence. The view that includes biglycan and decorin in the same subset of ubiquitous interstitial proteoglycans of the extracellular matrix of connective tissues needs partial revision on the basis of the data presented here. Whereas decorin seems to be a "full-time" matrix component, biglycan appears to be a cell surface or close territorial molecule (perhaps found

Figure 9. Detection of biglycan and decorin mRNAs in periosteal ossification. (**a,b**) Metaphyseal leading edge of periosteal ossification in the humerus. High levels of biglycan mRNA are detected in osteoblasts and osteocytes in the bony collar (bc). Strong hybridization signal is also observed in the inner (osteogenic) periosteum, whereas the outer (fibrous) periosteum (op) is virtually devoid of labeling. In contrast, the levels of decorin mRNA are comparable throughout the thickness of the periosteum, and high in bone cells. (**c,d**) Subperiosteal region of the mid-diaphysis of the humerus. Strong signal for (**c**) biglycan mRNA is seen in osteoblasts at the surfaces of bone trabeculae (bt) and in the innermost part of the periosteum. Osteoblasts on trabecular surfaces also show strong signal for decorin mRNA, as do fibroblasts in the periosteum (p). Bars = 60 μm.

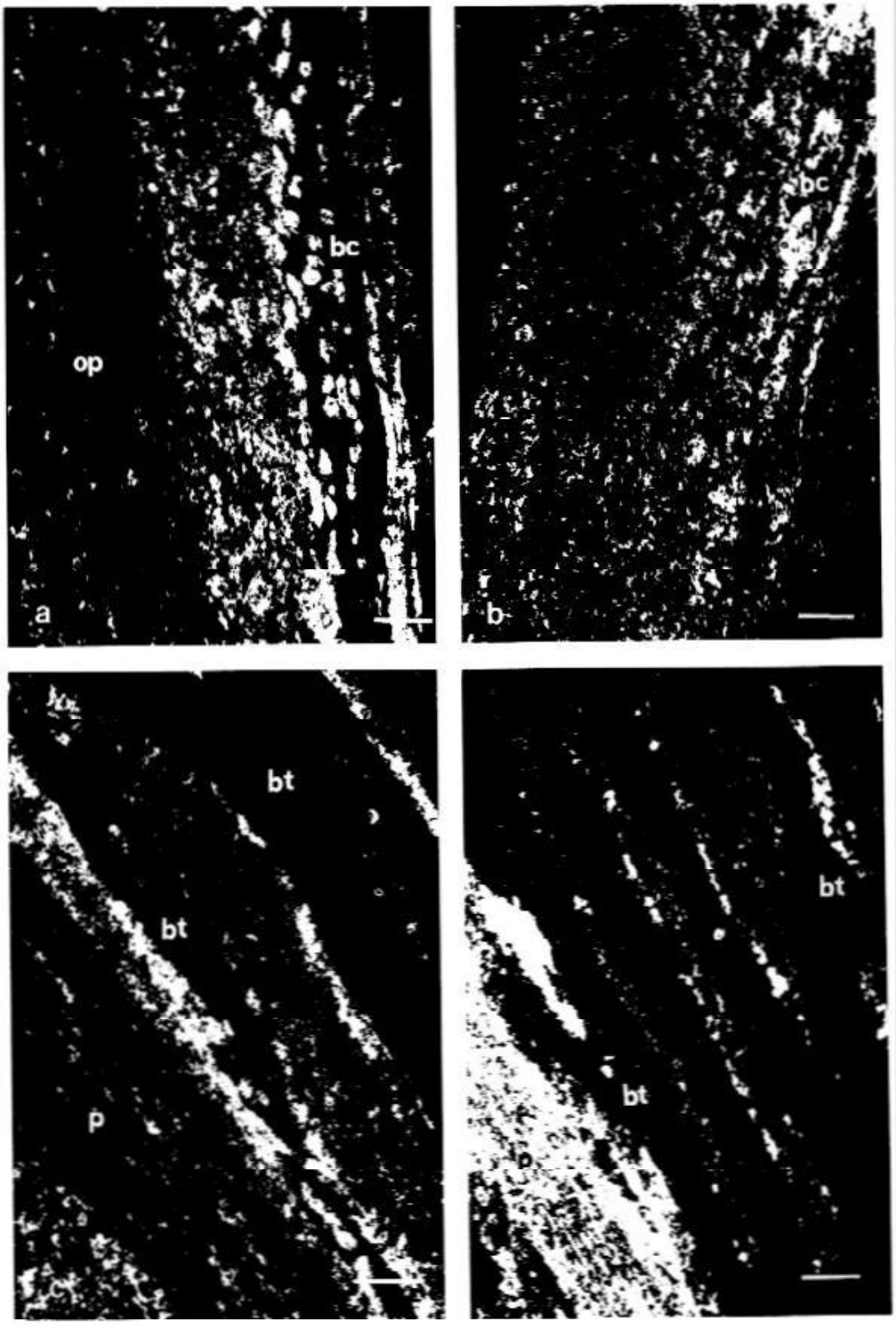
op
bc
a
bc
b
bt
bt
p
bt
bt
p

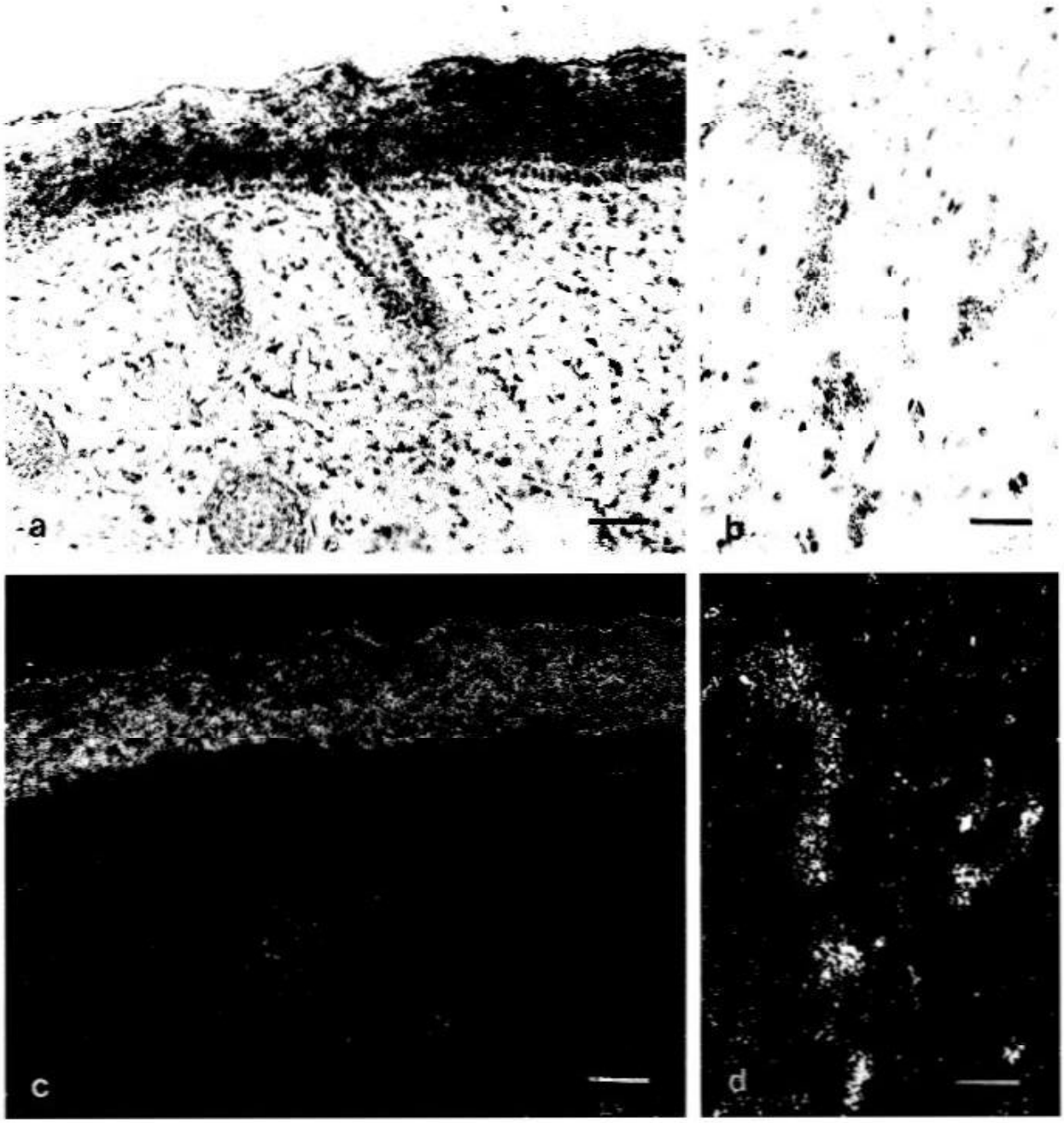

Figure 10. Biglycan mRNA in skin. (**a,b**) Brightfield and darkfield images showing strong hybridization signal over differentiating keratinocytes in the epidermis. Note the absence of significant signal in the dermis, over adnexae, and over the basal cell layer of the epidermis. (**c,d**) Brightfield and darkfield images of capillaries in the deep dermis, showing strong hybridization signal for biglycan mRNA. Bars: **a,b** = 40 μm; **c,d** = 20 μm.

Figure 11. Detection of biglycan and decorin mRNAs in developing kidney. (**a,b**) Brightfield and darkfield images of developing glomeruli in the cortex, showing hybridization signal for biglycan mRNA. (**c**) Low-power view of a kidney section hybridized with the decorin probe, showing strong signal over the interstitium, whereas tubular structures appear blank. (**d,e**) Brightfield and darkfield images of collecting tubules in the renal medulla, showing strong signal for biglycan. Bars: **a,b** = 100 μm; **c** = 180 μm; **d,e** = 140 μm.

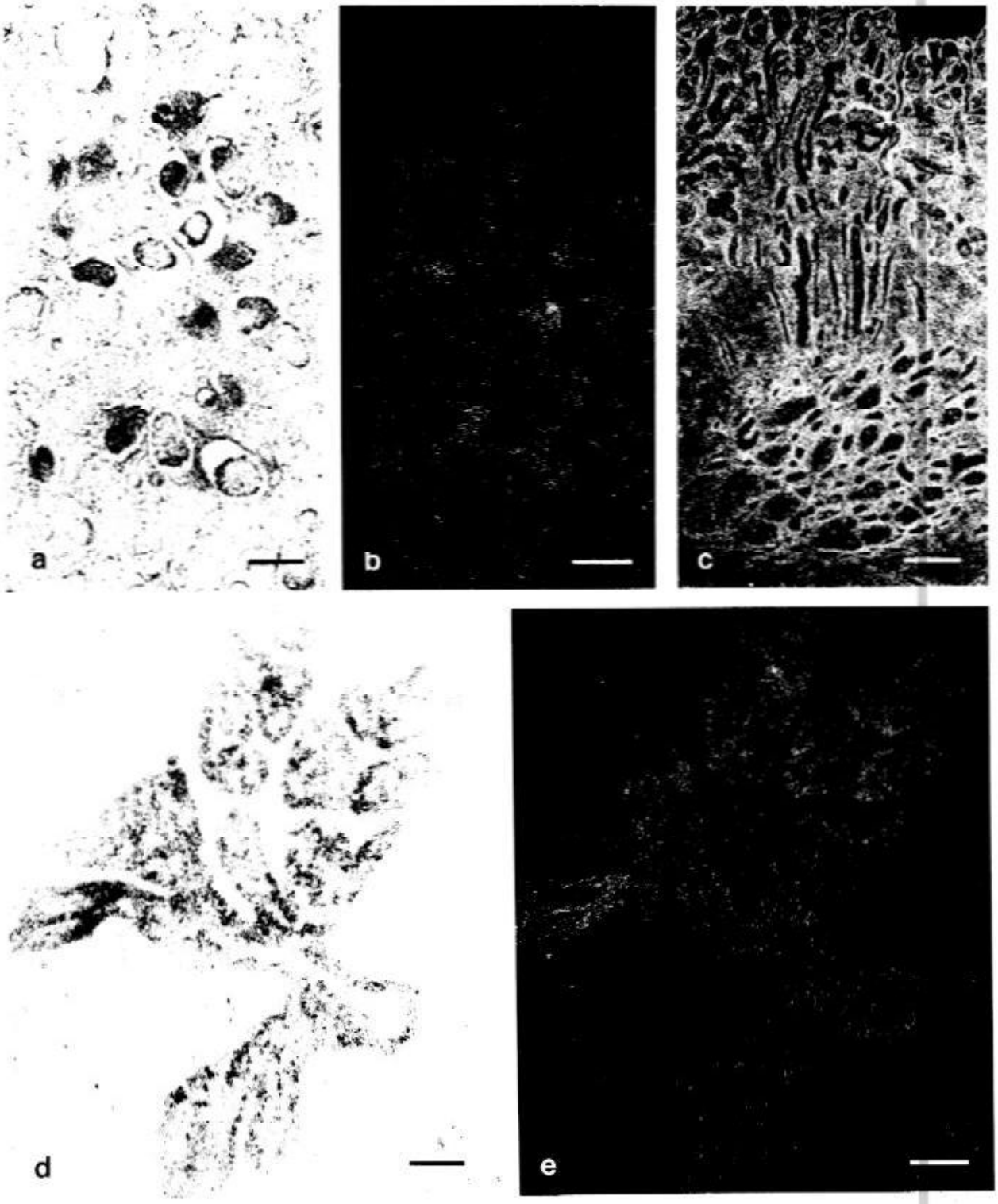
a
b
c
d
e

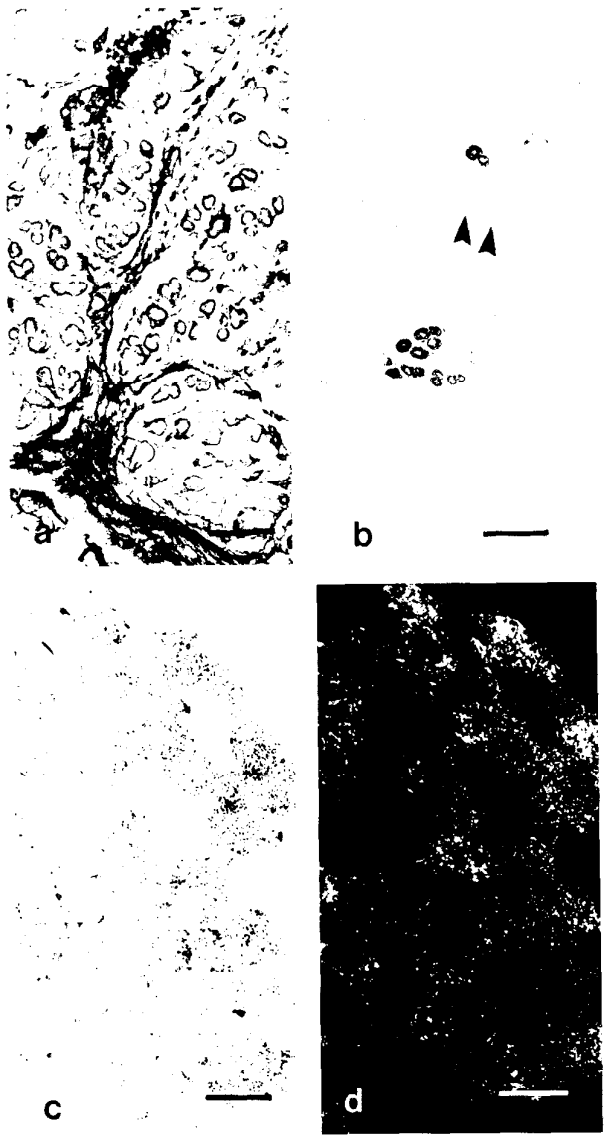

Figure 12. Biglycan and decorin in skeletal muscle. (**a**) Localization of decorin core protein in connective tissue sheaths. (**b**) Localization of biglycan core protein in individual skeletal myofibers. Connective tissue sheaths (arrowheads) are unstained. (**c,d**) Brightfield and darkfield images of skeletal myofibers displaying hybridization signal for biglycan mRNA. Bars: **a,b** = 30 μm; **c,d** = 80 μm.

in the matrix only after being shed from the surface and thus enriched in some closely pericellular environments, such as in cartilage and bone) and is most likely involved in functions other than matrix production and assembly.

Acknowledgment

We wish to thank Rick Dreyfuss for skilled help with photographic work.

Literature Cited

1. Cox KH, DeLeon DV, Angerer LM, Angerer RC: Detection of mRNAs in sea urchin embryos by in situ hybridization using asymmetric RNA probes. Dev Biol 101:485, 1984
2. David G, Lories V, Heremans A, van der Scheuren B, Cassiman JJ, van der Berghe H: Membrane-associated chondroitin sulfate proteoglycans of human lung fibroblasts. J Cell Biol 108:1165, 1989
3. Day AA, Ramis CI, Fisher LW, Gehron Robey P, Termine JD, Young MF: Characterization of bone PG II cDNA and its relationship to PG II mRNA from other connective tissues. Nucleic Acids Res 14:9861, 1986
4. Fisher LW, Hawkins GR, Tuross N, Termine JD: Purification and partial characterization of small proteoglycans I and II, bone sialoproteins I and II, and osteonectin from the mineral compartment of developing human bone. J Biol Chem 262:9702, 1987
5. Fisher LW, Termine JD, Young MF: Deduced protein sequence of bone small proteoglycan I (biglycan) shows homology with proteoglycan II (decorin) and several nonconnective tissue proteins in a variety of species. J Biol Chem 264:4571, 1989
6. Graham RC, Karnovsky MJ: The early stages of absorption of horseradish peroxidase in the proximal tubules of mouse kidneys: ultrastructural cytochemistry by a new technique. J Histochem Cytochem 14:291, 1966
7. Hassell JR, Kimura JH, Hascall VC: Proteoglycan core protein families. Annu Rev Biochem 55:539, 1986
8. Heinegard D, Oldberg A: Structure and biology of noncollagenous macromolecules. FASEB J 3:2042, 1989
9. Heinegard D, Paulsson M: Structure and metabolism of proteoglycans. In Piez KA, Reddi AH, eds. Extracellular matrix biochemistry. New York, Elsevier, 1984, 277
10. Kinsella MG, Wight TN: Isolation and characterization of dermatan sulfate proteoglycans synthesized by cultured bovine aortic endothelial cells. J Biol Chem 263:19222, 1988
11. Krusius T, Ruoslahti E: Primary structure of an extracellular matrix proteoglycan core protein deduced from cloned cDNA. Proc Natl Acad Sci USA 83:7683, 1986
12. Kuettner KE, Pauli BU: Vascularity of cartilage. In Hall BK, ed. Cartilage. Vol 1. New York, Academic Press, 1983, 281
13. Lufti AM: Mode of growth, fate and functions of cartilage canals. J Anat 106:135, 1970
14. Mikuni-Takagaki Y, Cheng Y: Metalloproteinases in endochondral bone formation: appearance of tissue-inhibitor resistant metalloproteinases. Arch Biochem Biophys 259:576, 1987
15. Neame PJ, Choi H, Rosenberg LC: The primary structure of the core protein of the small, leucine-rich proteoglycan (PG I) from bovine articular cartilage. J Biol Chem 264:8653, 1989
16. Parthasarathy N, Tanzer ML: Isolation and characterization of a low molecular weight chondroitin sulfate proteoglycan from rabbit skeletal muscle. Biochemistry 26:3149, 1987
17. Poole AR, Webber C, Pidoux I, Choi H, Rosenberg LC: Localization of a dermatan sulfate proteoglycan (DS-PGII) in cartilage and the presence of an immunologically related species in other tissues. J Histochem Cytochem 34:619, 1986
18. Rahemtulla F, Moorer C, Wille JJ: Biosynthesis of proteoglycans by proliferating and differentiating normal human keratinocytes cultured in serum free medium. J Cell Physiol 140:98, 1989
19. Roughley PJ, White RJ: Dermatan sulfate proteoglycans of human articular cartilage. The properties of dermatan sulfate proteoglycans I and II. Biochem J 262:823, 1989
20. Ruoslahti E: Proteoglycans in cell regulation. J Biol Chem 264:13369, 1989

21. Ruoslahti E: Structure and biology of proteoglycans. Annu Rev Cell Biol 4:229, 1986

22. Sampaio L de O, Bayliss MT, Hardingham TE, Muir H: Dermatan sulfate proteoglycan from human articular cartilage. Variation in its content with age and its structural comparison with a small chondroitin sulfate proteoglycan from pig laryngeal cartilage. Biochem J 254:757, 1988

23. Scott JE, Haigh M: Proteoglycan-type I collagen fibril interactions in bone and noncalcifying connective tissues. Biosci Rep 5:71, 1985

24. Scott JE, Orford CR: Dermatan-sulfate rich proteoglycan associates with the rat tailtendon collagen at the d band in the gap region. Biochem J 197:213, 1981

25. Sobue M, Nakashima N, Fukatsu T, Nagasaka T, Katoh T, Ogura T, Takeuchi J: Production and characterization of monoclonal antibody to dermatan sulfate proteoglycan. J Histochem Cytochem 36:479, 1988

26. Vogel K, Paulsson M, Heinegard D: Specific inhibition of type I and type II collagen fibrillogenesis by the small proteoglycan of tendon. Biochem J 223:587, 1984

27. Voss B, Glossl J, Cully Z, Kresse H: Immunocytochemical investigation on the distribution of small chondroitin/dermatan sulfate proteoglycan in the human. J Histochem Cytochem 34:1013, 1986